Parasitology International 65 (2016) 668–676

Contents lists available at ScienceDirect

Parasitology International

journal homepage: www.elsevier.com/locate/parint

Proteomic analysis of *Aedes aegypti* midgut during post-embryonic development and of the female mosquitoes fed different diets

Kenner Morais Fernandes [a], Marcos Jorge de Magalhães-Júnior [b], Maria Cristina Baracat-Pereira [b], Gustavo Ferreira Martins [a,*]

[a] Departamento de Biologia Geral, Universidade Federal de Viçosa - UFV, 36571-900 Viçosa, Minas Gerais, Brazil
[b] Departamento de Bioquímica e Biologia Molecular, Universidade Federal de Viçosa - UFV, 36571-900 Viçosa, Minas Gerais, Brazil

ARTICLE INFO

Article history:
Received 26 August 2015
Received in revised form 26 August 2016
Accepted 27 August 2016
Available online 3 September 2016

Keywords:
Aedes aegypti
Development
Midgut
Mosquito
Proteome

ABSTRACT

In this work we analyzed protein expression in the *Aedes aegypti* midgut during the larval (fourth instar, L4), pupal, and adult stages [including newly emerged (NE), sugar-fed (SF) and blood-fed (BF) females]. Two-dimensional electrophoresis showed 13 spots in the midgut of larvae, 95 in the midgut of pupae, 90 in the midgut of NE, and 76 in the midgut of SF or BF females. In the larval midguts, high serpin expression was noted, while in the pupae, protein abundance was lower than in the NE, SF, and BF females. The spots related to proteins linked to energy production, protein metabolism, signaling, and transport were highly expressed in the NE stage, while spots related proteins involved in translation were abundant in SF and BF females. The differential abundance of proteins in the midgut of *A. aegypti* at different developmental stages supports the necessity for midgut development during immature stage followed by the necessity of proteins related to digestion in adults.

1. Introduction

The yellow fever mosquito *Stegomyia aegypti* (=*Aedes aegypti*) is associated with the living spaces of humans, and is the primary vector of the dengue virus, and other viruses such as Chikungunya (CHIK) [1]. In general, *A. aegypti* females require a bloodmeal for ovarian development and oviposition to occur. When female mosquito feeds on blood, it is temporarily stored in the midgut, where digestion, absorption of nutrients, and infection by blood-borne pathogens (including viruses) occurs [2].

The ingestion of blood causes significant morphological and biochemical changes in the midgut of the adult female mosquito, resulting in epithelial flattening and increased protein synthesis of the peritrophic matrix (PM) and digestive enzymes (e.g., trypsin) in the posterior region of the organ [3]. Studies investigating gene expression in the midgut of *A. aegypti* females at a post-transcriptional level have shown that 3 and 7 days after feeding on sugar or blood, females had a similar protein expression profile, except for defensin, which increase in expression after blood-feeding [4]. On the other hand, when infected with CHIK virus or Dengue virus type 2 (DENV-2), modified expressions of proteins associated with regulatory, metabolic and structural pathways in the midgut were noted [5]. Moreover, midgut proteins linked to DENV-2 infection, including enolase, beta-ARK, and cadherin that can act as receptors, and the elongation factor EF-1 alpha/Tu that is important for viral replication [6], have recently been identified.

During its life cycle *A. aegypti* move from an aquatic to a terrestrial environment, and during this passage, the midgut undergoes changes in morphology and gene expression. The midgut remodeling during metamorphosis includes the replacement of digestive cells in the larval epithelium during pupation by the digestive cells of the adult. These changes allow the insect to change its diet and it ceases to feed on microorganisms and decomposing detritus and begins to feed on plant sugars and/or blood [7–9]. In this study, protein profiles of the *A. aegypti* midgut in the larval, pupal, and adult stages (newly emerged and fed with sugar or blood) were studied. In addition, we examined the possible roles of these proteins during the mosquito life cycle and during feeding, which contribute to a better understanding of the working dynamics of the midgut under different feeding conditions.

2. Material and methods

2.1. Mosquitoes and protein extraction

A. aegypti specimens (PPCampos strain, Campos dos Goytacazes, Rio de Janeiro) were obtained from a colony maintained in the insectary of the Department of General Biology at Universidade Federal de Viçosa, Brazil. Insects were raised in plastic trays containing dechlorinated tap water and containing turtle feed as a food source (Reptolife®-Alcon). The insects were maintained under conditions of controlled

* Corresponding author.
E-mail address: gmartins@ufv.br (G.F. Martins).

http://dx.doi.org/10.1016/j.parint.2016.08.008
1383-5769/

temperature (25 ± 5 °C), relative humidity (60 ± 5%), and a defined photoperiod (12:12 light/dark).

Two-hundred mosquito specimens were used to study each stage: 4th instar larvae (L4), female pupae 24 h after ecdysis (pupa), newly emerged adult females (0 − 12 h) (NE), adult females 3–4 days old fed on sugar solution (10% sucrose) (SF), and females fed sugar and provided with a blood meal (BF) from mouse anesthetized with Dopalen (Ceva). The midguts were dissected in PBS (0.1 M sodium phosphate buffer, pH 7.2). For L4, the midguts were gently pressed with tweezers for the expulsion of the food bolus surrounded by the PM. The midguts of BF were dissected 24 h after the blood meal. In this case, the ingested blood surrounded by the PM was discarded, and only midguts with no residual blood were used in the experiments.

After dissection, the midguts were gently washed in PBS and transferred to 50 μL of PBS at 4 °C containing 1 mM thiourea, 1 mM benzamidine, and 1 mM phenylmethylsulfonyl fluoride (PMSF), sonicated three times on ice, and centrifuged at 14,000 × *g* for 10 min at 4 °C. To the supernatant, 150 μL of cold acetone was added and maintained at − 20 °C for 3 h. After this period, the material was centrifuged at 14,000 × *g* for 10 min at 4 °C. The resulting pellet was resuspended in 50 μL of solubilization solution, consisting of 7 M urea, 2% CHAPS (w/v), and 2 M thiourea, and protein concentration was quantified by the Bradford method using BSA as standard protein.

2.2. Two-dimensional electrophoresis (2-DE) and image analysis

The 2-DE was performed at the Proteomics and Protein Biochemistry Laboratory, Universidade Federal de Viçosa. Midguts were taken from each mosquito developmental stage, and three 2-DE gel (technical replicates) from a pool of 200 mosquitoes was done for each stage or feeding condition. Each Immobiline DryStrip pH 3–10, 7 cm (GE Healthcare) was hydrated for 16 h with 125 μL of a solution containing 85 μg protein added Destreak (GE Healthcare), 40 mM dithiothreitol (DTT), and 2% (v/v) IPG buffer pH 3–10 (GE Healthcare). Isoelectric focusing (IEF) was performed using the IPGphor3™ (GE Healthcare) system in accordance with the manufacturer's instructions.

After IEF, strips were reduced for 15 min in a 5 mL buffer solution containing 75 mM Tris-HCl pH 8.8, 1% DTT, 6 M urea, 30% glycerol (v/v), 2% SDS (w/v), and 0.002% (w/v) bromophenol blue, and then alkylated in the same buffer by substituting DTT with 2.5% iodoacetamide. The second dimension was performed using polyacrylamide gel, 12% T glycine-SDS-PAGE (Sodium dodecyl sulfate

Table 1
Proteins of *A. aegypti* midgut identified by MS/MS. NE — newly emerged adults; SF- sugar fed adults; BF — blood fed adults.

Spot	Code	Protein	Sequence	Ion Score/C.I. %	e-Value	% Sequence coverage	Protein Score/C.I.,%
L481	gi|157116805	Serine proteinase inhibitors (serpins)	FKIEFDLDLKETLEK	115/100	8e-10	4	161/100
L482	gi|157116805	Serine proteinase inhibitors (serpins)	FKIEFDLDLKETLEK	108/100	2e-06	9	166/100
			GFRSEAESVNFQDNTATAK	23/72			
P6	gi|108877579	Trypsin-like serine protease	YNNPQFHNDIALVK	58/100	2e-9	5	91/100
	gi|157113343	Trypsin-like serine protease	IVQHPQFSYSTIDYDYSLLK	62/100	1e-15	7	
NE1	gi|403182713	Glyceraldehyde 3-phosphate dehydrogenase	LISWYDNEFGYSNR	65/100	1e-09	7	119/100
			IQVFQERDPK	21/90			
NE3	gi|94468602	Catalase [*A. aegypti*]	IWPQAEFPLIPVGR	28/97	3e-12	5	77/99
			LFAYTDTHR				
NE34	gi|157113061	Calreticulin family	FFNDEENDKGLQTSQDAR	30/96	8e-13	4	82/100
NE37	gi|157131648	ATP synthase alpha, central domain.	EAYPGDVFYLHSR	55/100	5e-10	5	124/100
			TALAIDTIINQQR	45/100			
NE38	gi|157168005	WD40	FSPNHSNPIIVSAGWDR	61/100	3e-12	5	122/100
NE39	gi|108871874	Conserved domains on Citrate synthases	ALGVLASLVWDR	60/100	2e-07	5	129/100
			SGQVVPGYGHAVLR	32/98			
NE41	gi|157124666	Voltage-dependent anion channel (VDAC)	EFGGLIYQR	35/99	9e-04	3	72/99
NE44	gi|108871874	Citrate synthases	LPVVAATIYR	22/90	7e-05	4	43/100
			ALGLPIERPK	21/90			
NE47	gi|403182713	Glyceraldehyde 3-phosphate dehydrogenase	LISWYDNEFGYSNR	50/100	7e-10	4	50/100
NE58	gi|108884060	Protein disulfide isomerase (PDI)	FVTAQALPLIVDFSHETAQK	68/100	3e-14	4	149/100
NE59	gi|108881686	*F*1 ATP synthase beta	IINVIGEPIDER	21/90	8e-07	2	99/100
NE60	gi|157121051	Enolase	GNPTVEVDLVTDLGLFR	88/100	1e-12	9	191/100
			SGETEDTFIADLVVGLSTGQIK	57/100			
NE64	gi|157120956	Arginine or creatine kinase [*A. aegypti*]	AVQQQLIDDHFLFK	43/100	1e-08	6	125/100
			IPFSHHDR	32/97			
NE65	gi|301641424	Actin partial [*A. aegypti*]	SYELPDGQVITIGNER	68/100	3e-10	7	125/100
			GYSFTTTAER	64/100			
NE67	gi|108880329	Aldo-keto reductases (AKRs)	LVPITSAAGHPYHPFEKEEF	56/100	3e-15	6	56/100
NE68	gi|157114623	Pyridine nucleotide-disulfide oxidoreductase	DGSKQELEFDVLLVSVGR	79/100	8e-12	3	145/100
NE69	gi|108879763	Sugar kinase/HSP70/actin superfamily	SYELPDGQVITIGNER	36/98	1e-10	4	71/100
NE70	gi|108879763	Sugar kinase/HSP70/actin superfamily	SYELPDGQVITIGNER	63/100	4e-10	7	105/100
			IWHHTFYNELR	29/82			
NE71	gi|108872600	14-3-3 epsilon	LGLALNFSVFYYEILNSPDR	32/97	1e-07	12	63/98
			YLAEFATGDDRK	22/62			
NE72	gi|157114501	14-3-3 protein	LGLALNFSVFYYEILNSPDK	125/100	6e-15	8	147/100
NE75	gi|301641424	Actin partial [A. aegypti]	SYELPDGQVITIGNER	60/100	1e-10	7	88/100
NE76	gi|765339426	Glutathione S-transferase (GST)	LVTLNSEVIPFYLEKLDDIAR	83/100	2e-07	17	235/100
			FLLSYGNLPFDDIR	78/100			
BF16	gi|94468818	HSPA5	IEIESFYEGDDFSETLTR	34/99	4e-13	3	34/99
BF18	gi|157119815	V/A-type ATP synthase catalytic subunit A	RVGYYELVGEIIRL	41/99	5e-08	8	123/100
			RALDDFYDKNFQEFVPLRT	27/99			
			KFGYVFAVSGPVVTAERM	22/99			
BF25	gi|357604983	Alpha_tubulin	RNLDIERPTYTNLNRL	39/99	1e-19	9	105/100
			RFDGALNVDLTEFQTNLVPYPRI	25/99			
BF28	gi|301641424	Actin	KSYELPDGQVITIGNERF	27/99	4e-07	14	97/100
			kIWHHTFYNELRV	26/99			
BF30	gi|108882996	Enolase	RGNPTVEVDLKTAKGLFRA	30/99	4e-07	4	95/100
BF33	gi157103617	Translation_Factor_II_like superfamily	R.AGQVGYLVCNMRTV.E	21/99	1e-03	2	92/100

Table 2
Proteins of *A. aegypti* midgut identified by MS. NE — newly emerged adults; SF- sugar fed adults; BF — blood fed adults.

Spot	Code	Protein	Best protein mass	Protein score/C.I.,%
NE35	gi|108873332	Glutamate dehydrogenase	251546	66/99
NE48	gi|157113865	RabGEF	238150	68/99
SF46	gi|357606304	ATP synthase	59495	129/100
BF40	gi|108876659	Trypsin-like serine protease	29844	78/100
BF54	gi|332023250	F1 ATP synthase alpha, central domain	59389	79/100
BF55	gi|32187519	Elongation factor 1-alpha (EF1-alpha)	32292	62/96
BF58	gi|108871015	Aspartate aminotransferase (AAT); provisional	39559	55/83

polyacrylamide gel electrophoresis), according to Laemmli [10]. The proteins were visualized using Coomassie Brilliant Blue staining (CBB) G-250 [11]. The 2-DE gels were scanned at 300 dpi using Image Scanner III (GE Healthcare) and analyzed by Image Master III (GE Healthcare), which identifies and quantifies the intensity of % volume protein spot.

2.3. Mass spectrometry

The gel plugs (here called protein spots or simply spots) were cut from the gels and their identification was performed at the Aveiro University Mass Spectrometry Center (Aveiro, Portugal), where the spots of interest were washed three times with 25 mM ammonium bicarbonate/50% (v/v) acetonitrile (ACN), once with ACN, and dried using SpeedVac (Thermo Savant). To the dried gel plugs, 25 μL of cleavage solution containing 10 ng/μL porcine trypsin (Promega) in 40 mM ammonium bicarbonate and 10% (v/v) of the ACN was added, and samples were incubated for 16 h at 37 °C.

Extraction of the trypsinized peptides was performed individually by three washes adding 5% (v/v) formic acid (FA)/50% ACN three times (30 min), generating three separate samples. The extracted samples (in FA) were pooled and lyophilized together within microcentrifuge tubes (500 μL). The peptides were then resuspended in 10 μL 0.1% FA/50% ACN. Samples were mixed (1:1) with the α-cyano-4-hydroxycinnamic acid matrix prepared in 50% ACN/0.1% FA. The mass spectra of the peptides were obtained using a mass spectrometer MALDI-TOF/TOF (4800 Proteomics Analyzer, Ab Sciex, Europe) in positive mode for the mass range 800–4500 Da. The mass spectra were calibrated internally using trypsin autodigestion peaks. Trypsin, human keratin and α-cyano-4-hydroxycinnamic acid matrix peaks were discarded from the mass spectra.

2.4. Protein identification

The obtained spectra were processed and analyzed by Global Protein Server Workstation (Applied Biosystems), using the MASCOT search algorithm (Matrix Science). The mass tolerance was 25 ppm, and the fragment ion mass tolerance was 0.3 Da. Positive identifications were accepted up to a 90% confidence level.

The identified proteins were clustered in six categories: proteins related to translation, cellular detoxification, energy production, protein and amino acid metabolism, signaling and transport, and cytoskeleton, besides those with unknown function.

2.5. Normalization

For comparison of relative protein abundance, gel spots identified from SF and BF were normalized against the spot[*s*] for the housekeeping protein tubulin (BF25), which showed similar volumes in mosquitoes under different diet conditions (SF or BF). The normalization was performed dividing the intensity values of the spots of SF or BF individually by the respective intensity value of tubulin [12]. Thereafter, the normalized spot intensities were divided between SF and BF, being accepted as differentially expressed spots with 50% difference in intensity % volume (BF > 1.5, SF < 0.6) (Sup. Table 1).

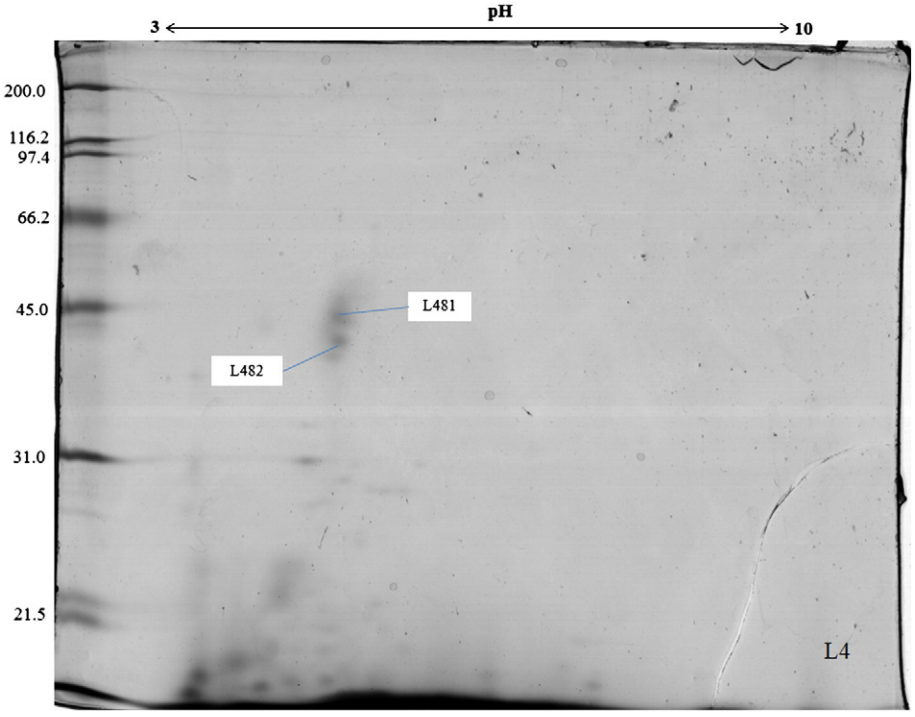

Fig. 1. Two-dimensional profile of the proteins extracted from 4th larvae (L4) midgut of *A. aegypti*. Identified spots are indicated. The numbers on the right side indicate the molecular mass standards in kDa.

2.6. Interactome construction

A network viewer program, Cytoscape (v3.0.2) (http://www.cytoscape.org), was used to build an "interactome", which we imported from a protein-protein interactions network from Intact (http was used.ac.uk/intact/). The Cytoscape program is connected to online databases, allowing networks of interacting proteins from the *Drosophila melanogaster* database to be imported.

A Cytoscape plug-in, ClueGO, was used to obtain biological terms for the protein interaction networks [13,14], which demonstrates the specificity and common aspects of the biological role of each protein, by using the most recent archives from Gene Ontology (http://www.geneontology.org/), KEGG (http://www.genome.jp/kegg/), and Reactome (http://www.reactome.org/). The biological roles of interactome proteins were identified by ClueGO, which was used to find the GOterm and GOannotations.

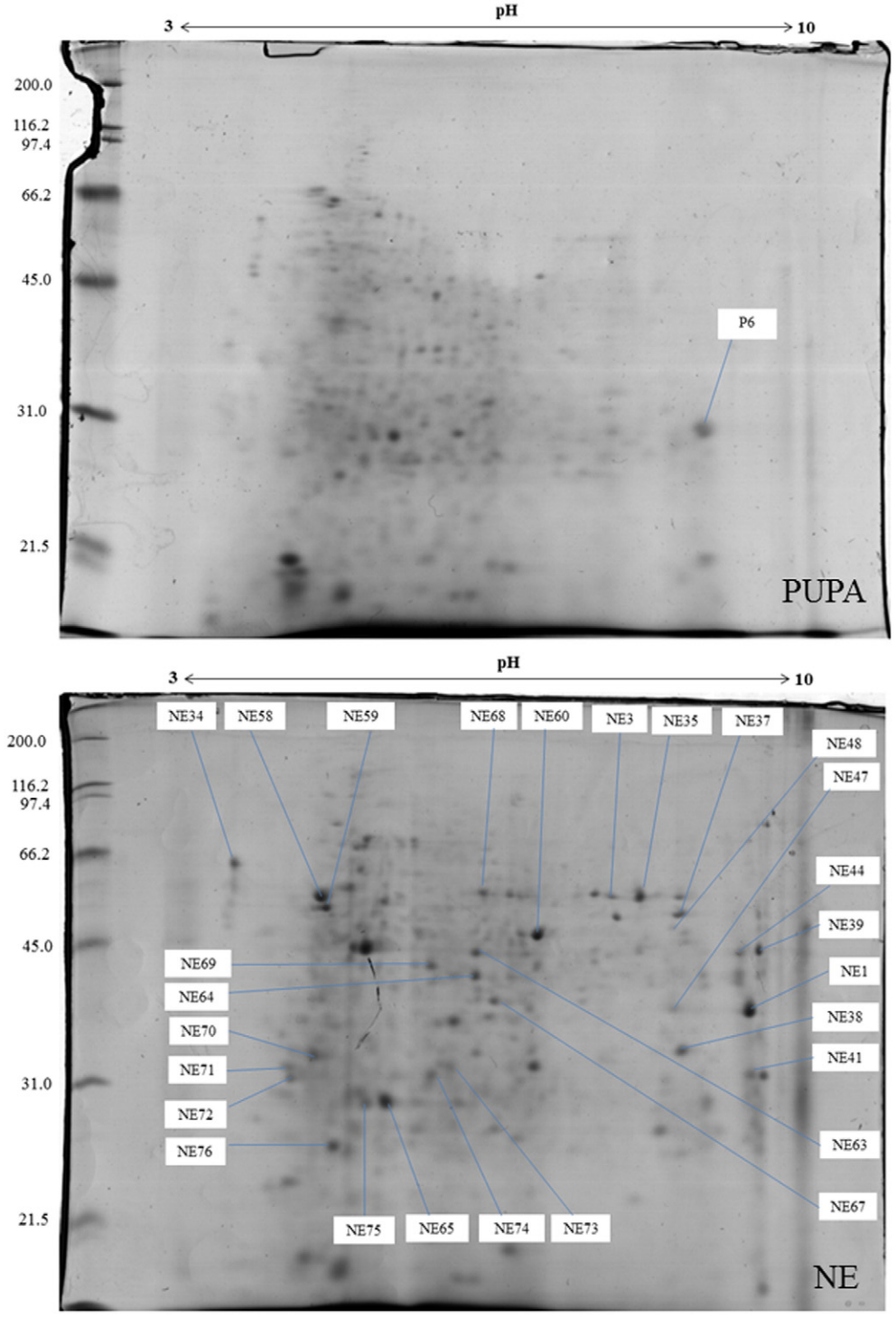

Fig. 2. Two-dimensional profiles of the proteins extracted from the midguts of pupa and newly emerged (NE) *A. aegypti* (females). Identified spots are indicated. The numbers on the right side indicate the molecular mass standards in kDa.

3. Results and discussion

By using 7-cm gels loaded with 85 μg of protein, 13 spots were detected in L4, 95 in pupae, 90 in NE, and 76 in SF or BF samples (274 spots in total). Thirty eight spots of 274 (approximately 13.8% of all spots) were identified by MS and MS-MS (Tables 1 and 2). There were only a few spots up above 20 kDa in the gels containing L4 samples, which made it impossible to make a comparative analysis with the other gels, limiting the analysis to pupae and adults (NE, SF, and BF). However, many spots were visualized below 21.5 kDa in L4 (Fig. 1). There were cases in which spots were identified corresponding to the same protein, such as NE37, NE59, SF46, and BF54. These proteins

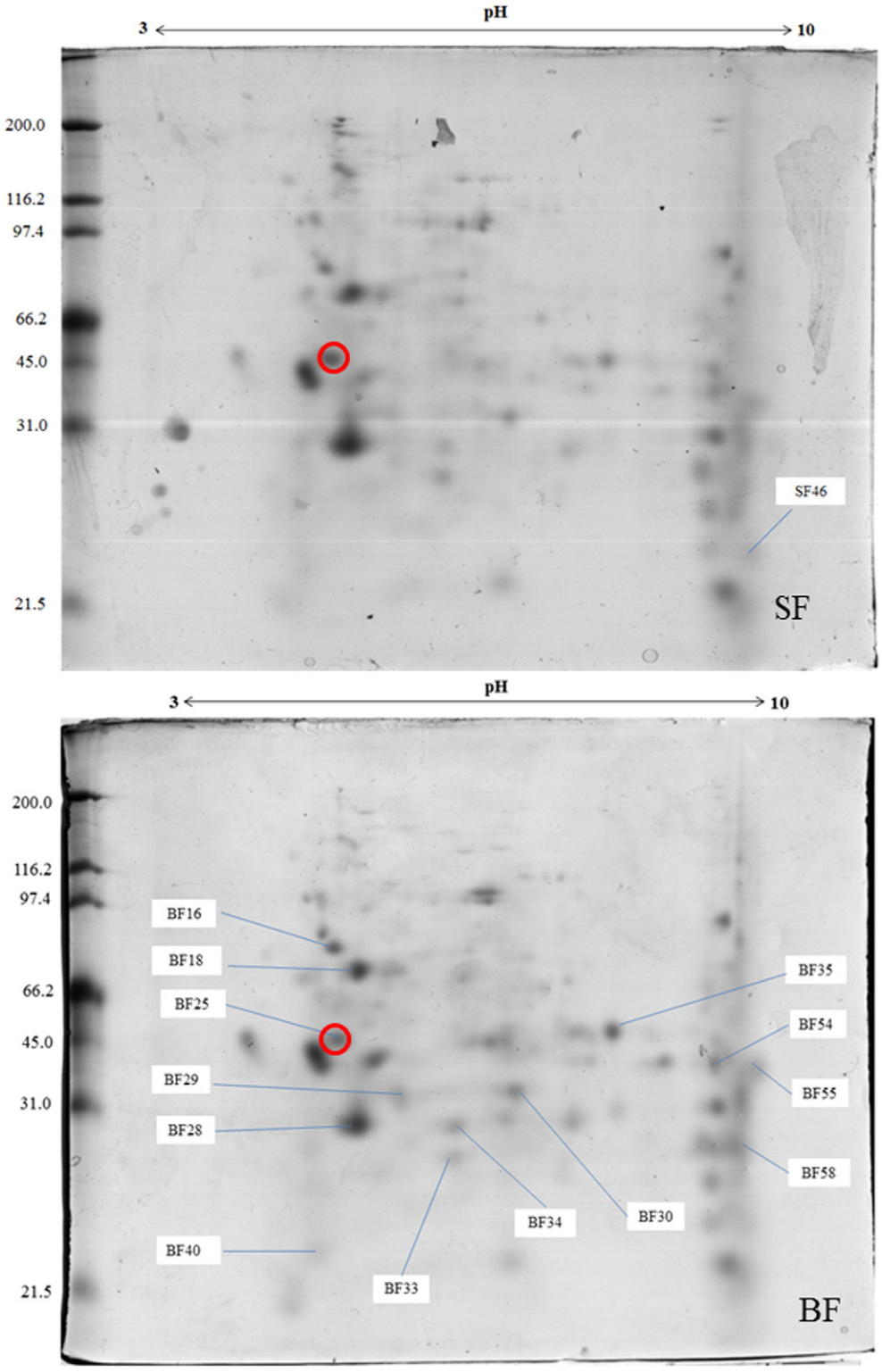

Fig. 3. Two-dimensional profiles of the proteins extracted from the midgut of sugar fed (SF) and blood fed (BF) *A. aegypti* adult females. Identified spots are indicated. The red circles point the tubulin (BF25) spots used for normalization. The numbers on the right side indicate the molecular mass standards in kDa.

probably are multiple members of these protein groups, and this could be due to post translational modifications, or isoforms, as has been observed in in the midgut of *A. aegypti* by 2-DE [5].

The profiles for pupae or NE were similar and consistent with that observed between the SF and BF groups. SF and BF had fewer spots in relation to NE and pupae, some of which had higher volume, with isoelectric points ranging from 3 to 6 (Figs. 2 and 3).

Gel analysis permitted comparisons to be made between samples for each protein identified, and relative quantitation could be performed according to the volume of the gel spots (Table 3). The gels of each sample were compared considering the quantity and volume of spots identified by CBB G-250 staining.

Three proteins involved in translation were identified: HspA5 (BF16), lepA_II (EF4; BF33), and EF1 (BF55). The spots related to these proteins were abundant in the BF. The results for HspA5 protein (isoform of the Hsp70 chaperone) [15] corroborates data found during blood feeding in the *A. aegypti* midgut, where there is an increase in the gene expression of Hsp70 in response to stress [16]. However, little is known about the function of elongation factor 4 (EF4), but it is considered essential for protein synthesis and cell viability due to its homology to EF1 [17,18], which increases its expression in the *A. aegypti* midgut following infection with DENV-2, suggesting that it may assist in viral replication [6].

Four proteins associated with detoxification were found: catalase (NE3), aldo keto reductase (AKRs; NE67), pyridine nucleotide-disulfide oxidoreductase (NE68), and glutathione S-transferase (GST; NE76). The spots related to these proteins were absent in pupae. Moreover, the spot related to catalase was not detected in BF or SF, while the pyridine nucleotide-disulfide oxidoreductase was not detected in SF. Antioxidant enzymes, such as catalase, GST, AKR and pyridine nucleotide-disulfide oxidoreductase are essential for cellular defense, which explains why their expression also is high in the adult *A. aegypti* midgut during infection with DENV-2 and CHIKV [5].

Eleven proteins related to energy production were identified, four of them corresponding to *F*1 ATP synthase (NE37, NE59, SF46 and BF54), two to glyceraldehyde-3-phosphate dehydrogenases (GAPDH; NE1 and NE47), two to citrate synthases (NE39 and NE44), two to enolases (NE60 and BF30) and creatine kinase (NE64).

Overall, it was remarkable the low expression of proteins associated with ATP production (ATP synthase) [19] and glycolysis (GAPDH, creatine kinase, enolase, and citrate synthase) [20–22] in pupae, which expressed only two spots, corresponding to ATP synthase (SF46) and enolase (BF30). In pupae, midgut epithelium is formed by cells in differentiation, with few organelles and consequently low metabolism [9]. In addition, the high expression of ATP synthase can influence the defensive system of the midgut of adult *A. aegypti* against pathogens [23]. Differently of adults, pupae do not feed and are less susceptible to infections.

Eight proteins involved in the metabolism of proteins and amino acids were identified: glutamate dehydrogenase (NE35), protein disulfide isomerase (PDI; NE58), aspartate aminotransferase (BF58), two serine protease inhibitors (serpins; L81 and L82), two serine proteases (trypsins; BF40 and *P*6) and one calreticulin (NE34). The spot corresponding to glutamate dehydrogenase (NE35) and calreticulin (NE34) were detected only in the NE midguts; whereas PDI and aspartate aminotransferase were absent or lower in the pupae, respectively. The serine protease corresponding to the spot BF40 were detected only in the NE and BF, while the spot *P*6 was abundant in the pupae.

The volume of two spots of L4 were higher than in the other stages (pupal and adults), and these were both identified as serpins (Fig. 1). Trypsin serine protease is also expressed in the midgut of pupae and NE, even if feeding does not occur during these stages. Besides acting in the bloodmeal digestion [24], midgut serine proteases may inhibit DENV-2 infection in *A. aegypti*, with an important role in the immune system of the mosquito [25]. While the pupal, NE, SF and BF midguts express trypsin, L4 expresses serpin in high quantities. In the mosquitoes *Anopheles stephensi* and *Anopheles gambiae*, serpin is involved in the midgut of the defense system during the invasion of *Plasmodium*, promoting lysis of the parasite [26].

Four other proteins related to protein metabolism were abundant in the NE and BF: glutamate dehydrogenase, aspartate aminotransferase, PDI and calreticulin [20,27–29]. Calreticulin and PDI are highly expressed during DENV-2 and CHIKV infection of the midgut, respectively, may be involved in the replication, translation, and/or viral encapsidation [5,30].

Table 3
Mean volume percentage of spots analyzed by the Image Master III software. Comparison of spots at different developmental stages of the *A. aegypti* midgut (pupa, NE, SF, and BF).

Match ID	BF	SF	NE	Pupa (24–48h)
Proteins related to translation				
BF16 — HspA5	1.12659	0.568875	0.364471	0.262127
BF33 — lepA_II (EF4)	0.894248	0.639274	0.431927	0.426204
BF55 — EF1	1.59567	0.981775	0.428591	0.109694
Proteins related to detoxification				
NE3 — Catalase	–	–	0.562832	–
NE67 — Aldo keto reductase (AKRs)	0.0963653	0.0853144	0.240702	–
NE68 — Pyridine nucleotide-disulfide oxidoreductase	0.157628	–	0.255305	–
NE76 — Glutathione *S*-transferase (GST)	0.127446	0.127028	0.407231	–
Proteins related to energy production				
NE1 — Glyceraldehyde-3-phosphate dehydrogenases (GAPDH)	0.302697	0.242194	0.948072	–
NE37 — F1 ATP synthase	–	–	0.198129	–
NE39 — Citrate synthases	0.100957	0.0935409	0.179817	–
NE44 — Citrate synthases	0.210682	0.136653	0.208107	–
NE47 — Glyceraldehyde-3-phosphate dehydrogenases (GAPDH)	0.302697	0.242194	0.748072	–
NE59 — F1 ATP synthase	–	–	0.446365	–
NE60 — Enolase	0.0912674	–	0.562832	–
NE64 — Creatine kinase	0.0858595	–	0.385595	–
SF46 — F1 ATP synthase	0.813864	0.715396	0.482325	0.247242
BF30 — Enolase	0.613993	0.574382	–	0.0931414
BF54 — F1 ATP synthase	0.872969	0.591193	0.116124	–
Proteins related to protein and amino acid metabolism				
NE34 — Calreticulin	–	–	0.368202	–
NE35 — Glutamate dehydrogenase	–	–	0.391126	–
NE58 — Protein disulfide isomerase (PDI)	0.151209	0.148265	0.920635	–
BF40 — Serine proteases	0.168127	–	0.156469	–
BF58 — Aspartate aminotransferase	0.925753	0.688312	0.817426	0.124883
P6 — Serine proteases	0.168127	0.11078	0.256469	0.788808
Proteins related to signaling and transport				
NE38 — WD40-repeat	–	0.0922369	0.31038	–
NE41 — Voltage dependent ion channels (VDAC)	0.251298	0.315405	0.239246	–
NE48 — RabGEF	–	–	0.142612	–
NE71 — 14-3-3 protein epsilon	–	–	0.20905	–
NE72 — 14-3-3 protein	–	–	0.224835	–
BF18 — V-ATPase	2.56825	1.84284	1.93819	0.33856
Proteins related to the constitution of the cytoskeleton and with unknown function				
NE65/BF28 — Actin	3.46902	2.91058	1.02502	0.532095
NE69 — Actin/hexokinase/HSP70 superfamily	0.0881993	–	0.258322	0.10113
NE70 — Actin/hexokinase/HSP70 superfamily	0.201968	0.124514	0.426368	–
NE75 — Actin	0.99019	0.610815	0.696299	0.224962
BF25 — Tubulin	3.46902	3.91058	1.902502	–

Three proteins involved in cell signaling - 14-3-3 protein (NE72), 14–3-3 protein epsilon (YWHAE; NE71), and WD40-repeat (NE38) - were identified, as well as proteins involved in transport: RabGEF (NE48), proteins that form voltage dependent ion channels (VDAC; NE41) and V-ATPase (BF18). The spot corresponding to the signaling proteins 14-3-3, 14-3-3 epsilon and the transport protein RabGEF were expressed only in the NE, while WD40 was detected in SF and NE midguts. However, the spots related to VDAC or V-ATPase were absent or lower in pupae, respectively.

Consistent with enzymes that are linked to protection, energy production, and protein metabolism, proteins that participate in signaling and transport (14-3-3 and WD40) [31,32] were also abundant in the NE. Interestingly, in the *A. aegypti* larvae midguts infected with CHIKV, WD-repeat proteins were highly expressed [5], while expression of 14-3-3 proteins was low in the midgut of mosquitoes infected with DENV-2 [30].

V-ATPase are proton pumps responsible for organelle acidification, in addition to being related to ATP hydrolysis and alkalinization of the anterior region of the lumen in the *A. aegypti* midgut [19,33–35]. Although the spots corresponding to VDAC and V-ATPase proteins are abundant in the adults, the spot corresponding to RabGEF' spot (regulate Rab GTPase) [36], was present only in the NE midgut.

Four spots corresponding to actin (NE65/BF28 and NE75) and tubulin (BF25) were identified and their volumes were lower and absent in the pupae midgut. Two proteins (NE69 and NE70) from different families but possessing a common domain referred to as the Actin/Hexokinase/HSP70 superfamily were identified. The volumes of spots corresponding to proteins NE69 and NE70 were absent in the SF and pupae midgut, respectively.

The in silico protein interaction analyses of the *A. aegypti* midgut resulted in 533 proteins with 1700 protein-protein interactions (Fig. 4 and Sup. Table 2). Furthermore, the proteins that constitute the interactome have 284 GOterm, originated from *D. melanogaster* databases by using the ClueGO application (Sup. Table 3). These proteins were distributed in the same six functional groups previously described: translation (EF1 and Hsp70), detoxification (catalase and GST), energy production (ATP synthase, glyceraldehyde-3-phosphate dehydrogenase, citrate synthase, enolase, and creatine kinase), protein and amino acid

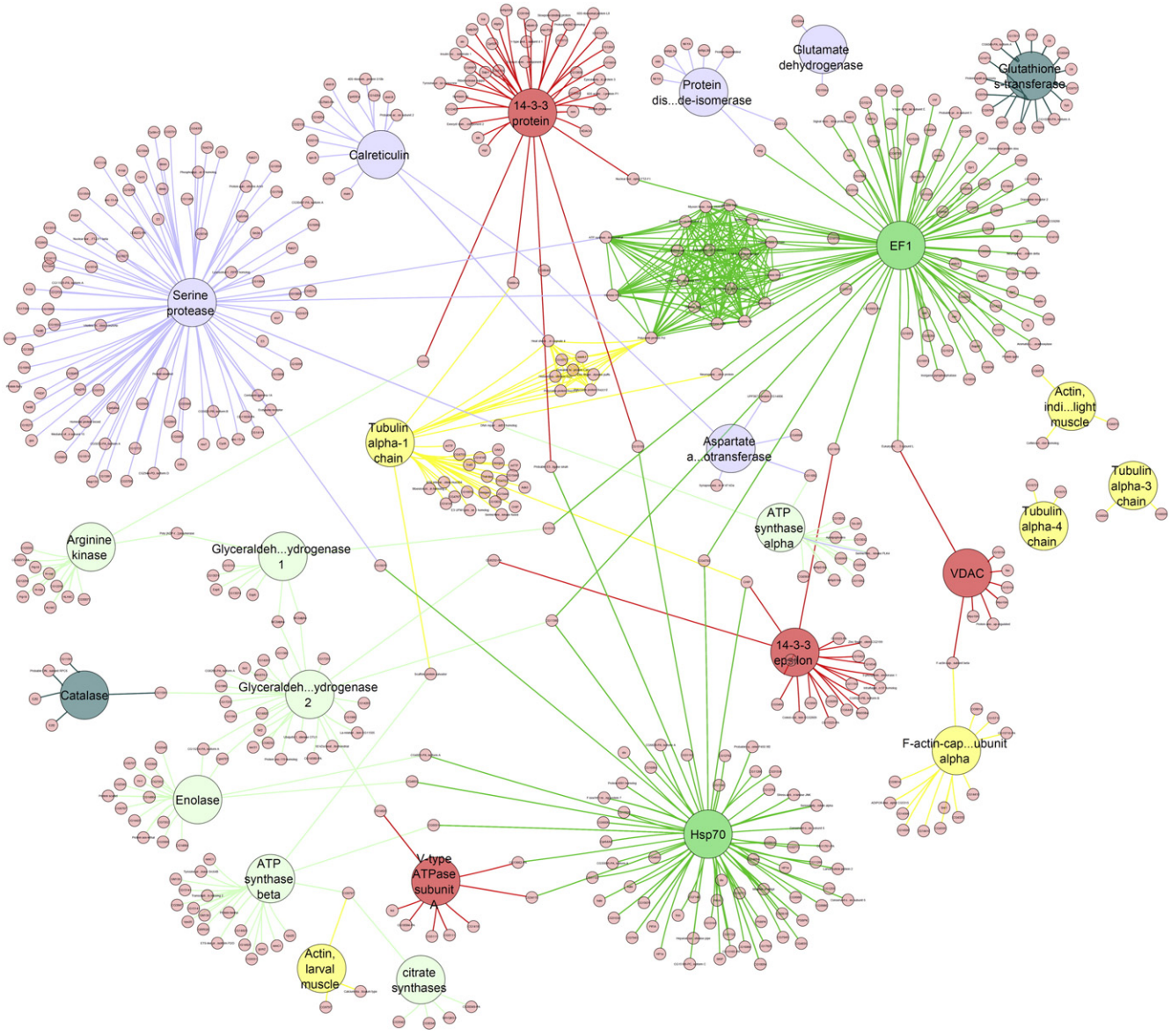

Fig. 4. Protein-protein interaction networks generated by Intact and visualized with Cytoscape (v3.0.2). This network consist of 533 proteins (nodes) connected by 1700 interactions (edges). These proteins are separated in six functional groups: translation (green), protein and aminoacid metabolism (purple), signaling and transport (red) and cytoskeleton (yellow).

metabolism (glutamate dehydrogenase, protein disulfide isomerase [PDI], aspartate aminotransferase, serine protease inhibitor [serpin], serine protease trypsin, and calreticulin), signaling and transport (14-3-3 protein, 14-3-3 protein epsilon, VDAC and V-ATPase) and cytoskeleton (actin and tubulin) (Fig. 4). Four proteins, EF4, AKR, WD40-repeat and RabGEF were not analyzed, because there were no interaction networks available in the *D. melanogaster* database; HspA5 was replaced using Hsp70, because they are isoforms. The fruit fly corresponding proteins found in the mosquito midgut are listed in the Sup. Table 4.

The interactome revealed the complexity of protein-protein interactions in the *A. aegypti* midgut. For example, the translation proteins EF1 and Hsp70 interact with 166 different proteins, many of which are common to other identified proteins and are related to response pathways involved in cellular stress in *D. melanogaster* [37,38].

Catalase also participates in the response to cell stress, but acts via distinct EF1 and Hsp70 pathways by interacting with the transcription factor E2F2, which may be a C6 subunit of RNA polymerase III and the CG11581 protein, of unknown function. On the other hand, GST interacts with 16 different proteins, none of which interacts with any other proteins that make up the interactome. This shows that even though GST has the same antioxidant function as catalase, the routes of action of these two proteins are distinct. The fact that catalase and GST act in different ways could explain why in the *A. aegypti* midgut, catalase was highly expressed during DENV-2 infection, whereas GST was highly expressed during CHIKV infection [5], demonstrating that each pathway is activated in a virus-dependent manner.

Three proteins that were abundant in the NE are calreticulin, 14-3-3 protein (a family of conserved regulatory molecules), and 14-3-3 protein epsilon, which together interact with 72 different proteins, most of which are involved in the developmental processes (Table 3). In *D. melanogaster*, calreticulin is important for nervous system development, in olfaction and, in the regulation of "sleep" [39–44]. Conversely, 14-3-3 protein and 14-3-3 protein epsilon are essential for oocyte development and differentiation, growth control, apoptosis, and longevity [45–47]. The expression of these three proteins in the NE midgut suggest that these proteins may be important in the final stage of the post-embryonic development of the *A. aegypti* midgut.

4. Conclusions

The synthesis of multiple proteins seems to be essential for the formation and constitution of the new midgut epithelium and that it begins in the midgut of the *A. aegypti* larvae. However, peak expression of some spots related to these proteins seems to occur at the end of development, corresponding to the NE stage. On the other hand, for the SF and BF groups, the protein profiles within the midgut were similar, and they demonstrated fewer spots than for both the pupae and NE groups.

Our study identified several expressed proteins in the *A. aegypti* midgut during development and feeding, which is an important step in understanding the organ biology of blood-sucking mosquitoes. Additionally, the interactome generated based on the identified proteins showed that they may be acting in little-known ways through complex networks of protein-protein interactions, and many of the proteins involved in these networks also have unknown functions. Finally, experiments aiming to interfere with differentially expressed proteins at different levels are required to fully determine the role of the protein repertoire in the development and feeding process of *A. aegypti*.

Supplementary data to this article can be found online at http://dx.doi.org/10.1016/j.parint.2016.08.008.

Acknowledgements

To Conselho Nacional de Desenvolvimento Científico e Tecnológico (CNPq, 480275/2011-4), Coordenação de Aperfeiçoamento de Pessoal de Nível Superior (CAPES/PVE 88881.030429/2013-01) and Fundação Arthur Bernardes (FUNARBE) for financial support.

References

[1] WHO, Yellow Fever Factsheet, World Health Organization, Geneva, 2001.
[2] W.C. Black, K.E. Bennett, N. Gorrochótegui-Escalante, C.V. Barillas-Mury, I. Fernández-Salas, M. de Lourdes Muñoz, J.A. Farfán-Alé, K.E. Olson, B.J. Beaty, Flavivirus susceptibility in *Aedes aegypti*, Arch. Med. Res. 33 (2002) 379–388.
[3] P.F. Billingsley, The midgut ultrastructure of hematophagous insects, Annu. Rev. Entomol. 35 (1990) 219–248.
[4] L. Wasinpiyamongkol, S. Patramool, N. Luplertlop, P. Surasombatpattana, S. Doucoure, F. Mouchet, M. Séveno, F. Remoue, E. Demettre, J. Brizard, P. Jouin, D.G. Biron, F. Thomas, D. Missé, Blood-feeding and immunogenic *Aedes aegypti* saliva proteins, Proteomics 10 (2010) 1906–1916.
[5] S. Tchankouo-Nguetcheu, H. Khun, L. Pincet, P. Roux, M. Bahut, M. Huerre, C. Guette, V. Choumet, Differential protein modulation in midguts of *Aedes aegypti* infected with chikungunya and dengue 2 viruses, PLoS One 5 (2010) e13149.
[6] M.L. Muñoz, G. Limón-Camacho, R. Tovar, A. Diaz-Badillo, G. Mendoza-Hernández, W.C. Black IV, Proteomic identification of dengue virus binding proteins in *Aedes aegypti* mosquitoes and *Aedes albopictus* cells, Biomed. Res. Int. 2013 (2013).
[7] J.T. Nishiura, P. Ho, K. Ray, Methoprene interferes with mosquito midgut remodeling during metamorphosis, J. Med. Entomol. 40 (2003) 498–507.
[8] K. Ray, M. Mercedes, D. Chan, C.Y. Choi, J.T. Nishiura, Growth and differentiation of the larval mosquito midgut, J. Insect Sci. 9 (2009) 1–13.
[9] K.M. Fernandes, C.A. Neves, J.E. Serrão, G.F. Martins, *Aedes aegypti* midgut remodeling during metamorphosis, Parasitol. Int. 63 (2014) 506–512.
[10] U.K. Laemmli, Cleavage of structural proteins during assembly of the head of bacteriophage T4, Nature 227 (1970) 680–685.
[11] V. Neuhoff, R. Stamm, H. Eibl, Clear background and highly sensitive protein staining with Coomassie blue dyes in polyacrylamide gels: A systematic analysis, Electrophoresis 6 (1985) 427–448.
[12] S.P. Borgaonkar, H. Hocker, H. Shin, M.K. Markey, Comparison of normalization methods for the identification of biomarkers using MALDI-TOF and SELDI-TOF mass spectra, OMICS 14 (2010) 115–126.
[13] G. Bindea, B. Mlecnik, H. Hackl, P. Charoentong, M. Tosolini, ClueGO: a Cytoscape plug-in to decipher functionally grouped gene ontology and pathway annotation networks, Bioinformatics 25 (2009) 1091–1093.
[14] G. Bindea, J. Galon, B. Mlecnik, CluePedia Cytoscape plugin: pathway insights using integrated experimental and *in silico* data, Bioinformatics 29 (2013) 661–663.
[15] M. Wisniewska, T. Karlberg, L. Lehtio, I. Johansson, T. Kotenyova, M. Moche, H.S. Ler, Crystal structures of the ATPase domains of four human Hsp70 isoforms: HSPA1L/Hsp70-hom, HSPA2/Hsp70-2, HSPA6/Hsp70B, and HSPA5/BiP/GRP78, PLoS One 5 (2010) e8625.
[16] H.R. Sanders, A.M. Evans, L.S. Ross, S.S. Gill, Blood meal induces global changes in midgut gene expression in the disease vector, *Aedes aegypti*, Insect Biochem. Mol. Biol. 33 (11) (2003) 1105–1122.
[17] Y. Fan, M. Schlierf, A.C. Gaspar, C. Dreux, A. Kpebe, L. Chaney, A. Mathieu, C. Hitte, O. Grémy, E. Sarot, M. Horn, Y. Zhao, T.G. Kinzy, L. Rabinow, *Drosophila* translational elongation factor-1gamma is modified in response to DOA kinase activity and is essential for cellular viability, Genetics 184 (2010) 141–154.
[18] H. Liu, C. Chen, H. Zhang, J. Kaur, Y.E. Goldman, B.S. Cooperman, The conserved protein EF4 (LepA) modulates the elongation cycle of protein synthesis, Proc. Natl. Acad. Sci. U. S. A. 108 (39) (2011) 16223–16228.
[19] A. Popova-Butler, D.H. Dean, Proteomic analysis of the mosquito *Aedes aegypti* midgut brush border membrane vesicles, J. Insect Physiol. 55 (2009) 264–272.
[20] S.F. Altschul, T.L. Madden, A.A. Schäffer, J. Zhang, Z. Zhang, W. Miller, D.J. Lipman, Gapped BLAST and PSI-BLAST: a new generation of protein database search programs, Nucleic Acids Res. 25 (1997) 3389–3402.
[21] S.N. Thompson, Pyruvate cycling and implications for regulation of gluconeogenesis in the insect, *Manduca sexta* L, Biochem. Biophys. Res. Commun. 274 (2000) 787–793.
[22] J.W. Kim, C.V. Dang, Multifaceted roles of glycolytic enzymes, Trends Biochem. Sci. 30 (2005) 142–150.
[23] A. Cancino-Rodezno, L. Lozano, C. Oppert, J.I. Castro, H. Lanz-Mendoza, S. Encarnación, A.E. Evans, S.S. Gill, M. Soberón, J.L. Jurat-Fuentes, A. Bravo, Comparative proteomic analysis of *Aedes aegypti* larval midgut after intoxication with Cry11Aa toxin from *Bacillus thuringiensis*, PLoS One 7 (5) (2012) e37034.
[24] F.G. Noriega, X.Y. Wang, J.E. Pennington, C.V. Barillas-Mury, M.A. Wells, Early trypsin, a female-specific midgut protease in *Aedes aegypti*: isolation, amino-terminal sequence determination, and cloning and sequencing of the gene, Insect Biochem. Mol. Biol. 26 (2) (1996) 119–126.
[25] D.E. Brackney, B.D. Foy, K.E. Olson, The effects of midgut serine proteases on dengue virus type 2 infectivity of *Aedes aegypti*, Am.J.Trop. Med. Hyg. 79 (2) (2008) 267–274.
[26] E.G. Abraham, S.B. Pinto, A. Ghosh, D.L. Vanlandingham, A. Budd, S. Higgs, F.C. Kafatos, M. Jacobs-Lorena, K. Michel, An immune-responsive serpin, SRPN6, mediates mosquito defense against malaria parasites, Proc. Natl. Acad. Sci. 102 (45) (2005) 16327–16332.
[27] L. Saboia-Vahia, A. Borges-Veloso, P. Cuervo, M. Junqueira, C. Mesquita-Rodrigues, C. Britto, G.B. Domont, J.B. De Jesus, Protein expression in the midgut of sugar-fed *Aedes albopictus* females, Parasitol. Vectors 5 (2012) 290.
[28] B. Wilkinson, H.F. Gilbert, Protein disulfide isomerase, Biochim. Biophys. Acta 1699 (1) (2004) 35–44.
[29] J.M. Tarr, P.J. Young, R. Morse, D.J. Shaw, R. Haigh, P.G. Petrov, S.J. Johnson, P.G. Winyard, P.A. Eggleton, Mechanism of release of calreticulin from cells during apoptosis, J. Mol. Biol. 401 (2010) 799–812.
[30] M. Zhang, X. Zheng, Y. Wu, M. Gan, A. He, Z. Li, D. Zhang, X. Wu, X. Zhan, Differential proteomics of *Aedes albopictus* salivary gland, midgut and C6/36 cell induced by dengue virus infection, Virology 444 (2013) 109–118.

[31] P. Mhawech, 14-3-3 proteins - an update, Cell Res. 15 (2005) 228–236.
[32] C.U. Stirnimann, E. Petsalaki, R.B. Russell, C.W. Müller, WD40 proteins propel cellular networks, Trends Biochem. Sci. 35 (2010) 565–574.
[33] J.J. Lemasters, E. Holmuhamedov, Voltage-dependent anion channel (VDAC) as mitochondrial governator-thinking outside the box, Biochim. Biophys. Acta 1762 (2006) 181–190.
[34] H. Wieczorek, K.W. Beyenbach, M. Huss, O. Vitavska, Vacuolar-type proton pumps in insect epithelia, J. Exp. Biol. 212 (2009) 1611–1619.
[35] H. Onken, S.B. Moffett, D.F. Moffett, Alkalinization in the isolated and perfused anterior midgut of the larval mosquito, *Aedes aegypti*, J. Insect Sci. 8 (2008) 1–20.
[36] J. Blümer, J. Rey, L. Dehmelt, T. Mazel, Y.W. Wu, P. Bastiaens, R.S. Goody, RabGEFs are a major determinant for specific Rab membrane targeting, J. Cell Biol. 200 (2013) 287–300.
[37] F. Ponton, M.P. Chapuis, M. Pernice, G.A. Sword, S.J. Simpson, Evaluation of potential reference genes for reverse transcription-qPCR studies of physiological responses in *Drosophila melanogaster*, J. Insect Physiol. 57 (2011) 840–850.
[38] A.O. Abolaji, J.P. Kamdemb, T.H. Lugokenski, T.K. Nascimento, E.P. Waczuk, E.O. Farombi, E.L.S. Loreto, J.B.T. Rocha, Involvement of oxidative stress in 4-vinylcyclohexene-induced toxicity in *Drosophila melanogaster*, Free Radic. Biol. Med. 71 (2014) 99–108.
[39] S.N. Prokopenko, Y. He, Y. Lu, H.J. Bellen, Mutations affecting the development of the peripheral nervous system in *Drosophila*: a molecular screen for novel proteins, Genetics 156 (2000) 1691–1715.
[40] F. Bejarano, C.M. Luque, H. Herranz, G. Sorrosal, N. Rafel, T.T. Pham, M. Milán, A gain-of-function suppressor screen for genes involved in dorsal-ventral boundary formation in the *Drosophila* wing, Genetics 178 (2008) 307–323.
[41] S.T. Harbison, A. Sehgal, Quantitative genetic analysis of sleep in *Drosophila melanogaster*, Genetics 178 (2008) 2341–2360.
[42] A. Yamamoto, L. Zwarts, P. Callaerts, K. Norga, T.F.C. Mackay, R.R.H. Anholt, Neurogenetic networks for startle-induced locomotion in *Drosophila melanogaster*, Proc. Natl. Acad. Sci. U. S. A. 105 (2008) 12393–12398.
[43] V.P. Carreira, I.M. Soto, J. Mensch, J.J. Fanara, Genetic basis of wing morphogenesis in *Drosophila*: sexual dimorphism and non-allometric effects of shape variation, BMC Dev. Biol. 11 (2011) 32.
[44] S. Swarup, S.T. Harbison, L.E. Hahn, T.V. Morozova, A. Yamamoto, T.F.C. Mackay, R.R.H. Anholt, Extensive epistasis for olfactory behaviour, sleep and waking activity in *Drosophila melanogaster*, Genet. Res. 94 (2012) 9–20.
[45] R. Benton, I.M. Palacios, D. St Johnston, *Drosophila* 14-3-3/PAR-5 is an essential mediator of PAR-1 function in axis formation, Dev. Cell 3 (2002) 659–671.
[46] M.D. Nielsen, X. Luo, B. Biteau, K. Syverson, H. Jasper, 14-3-3 Epsilon antagonizes FoxO to control growth, apoptosis and longevity in *Drosophila*, Aging Cell 7 (2008) 688–699.
[47] K.K. Tsigkari, S.F. Acevedo, E.M.C. Skoulakis, 14-3-3ε is required for germ cell migration in *Drosophila*, PLoS One 7 (2012), e36702.